17th World Conference on Earthquake Engineering, 17WCEE
Sendai, Japan - September 13th to 18th 2020

SEISMIC EVALUATION OF JAPANESE TWO-ELEVATION INTEGRATED CEILING SYSTEM

Liangjie Qi[(1)], Keiichiro Kunitomo[(2)], Masahiro Kurata[(3)], Yoshiki Ikeda[(4)]

[(1)] *JSPS Postdoctoral Fellow, Disaster Prevention Research Institute, Kyoto University, qi.liangjie.76r@st.kyoto-u.ac.jp*
[(2)] *Graduate Student, Department of Architecture and Architectural Engineering, Kyoto University, kunitomo.keiichiro.84c@st.kyoto-u.ac.jp*
[(3)] *Associate Professor, Disaster Prevention Research Institute, Kyoto University, kurata.masahiro.5c@kyoto-u.ac.jp*
[(4)] *Professor, Disaster Prevention Research Institute, Kyoto University, ikeda.yoshiki.6r@kyoto-u.ac.jp*

Abstract

Recent earthquakes highlighted the vulnerability of nonstructural components and its tremendous impact on building usage. The suspended ceiling system and equipment are examples of frequently-damaged components. These components often interact during shaking under earthquakes, but their interactions are not well-studied. Also, most previous studies only focused on the responses and behavior of regular-shape ceiling, i.e., square and leveled. However, the ceiling height of two adjacent rooms may differ when the two rooms have different usage plans. In such cases, the ceiling has a two-elevation layout. The rise-up location is often temporarily reinforced for construction based on sub-constructor's judgment but their seismic behavior is not well-known.

To address such issues, the studies of the Japanese two-elevation integrated system, including ceiling and equipment, were conducted numerically and experimentally. First, the small-amplitude vibration tests of the integrated ceiling system considering the interactions with equipment (i.e., air-conditioners and lighting fixture) and peripheral constraint (as a representation of surrounding walls) were conducted. The test results showed that the inclusion of peripheral constraints increased the first horizontal vibration frequency of the ceiling system by a factor of six. The natural frequencies of all components in the integrated ceiling system were almost identical, which was attributed to the coupled behavior between the ceiling panels and surrounding equipment, emphasizing the effect of interactions between adjacent components under dynamic excitation.

To better understand the seismic behavior of the two-elevation integrated ceiling system, shake table tests and the corresponding numerical studies were performed subsequently. The studies aimed to examine the coupled behavior of ceiling panels surrounded by equipment and the influence of the reinforcing bars at the rise-up location. The damage sequence of the integrated ceiling system subjected to the JMA Kobe ground motion, whose PGV was scaled at 50 cm/s, was identified as follows: First, the sliding of the air conditioners (ACs) and lighting fixtures occurred, and this phenomenon lasted for the subsequent excitation period. However, the collision was only present between lighting fixtures and the panels because of the insufficient clearance around the lighting fixtures. Then, the stresses on the vertical suspension bars of ACs connecting with the diagonal braces exceeded the yield stress, followed by the yielding of two ends of suspension bars on the higher elevation. From the results of shake table tests, the temporarily reinforcing bars connecting two ceiling layers are beneficial to reduce the relative displacement and ensure the integrity of the integrated ceiling system, and such members should be installed regardless of member sections in the Japanese two-elevation integrated ceiling system.

Keywords: Integrated ceiling systems; electric equipment; vibration test; shake table test; seismic evaluation

1. Introduction

The suspended ceilings and electric equipment are vulnerable to collision and falling failure when buildings are subjected to earthquakes, leading to immeasurable economic loss and disturbance of the timely rescue of casualty. For example, because the design requirements for nonstructural components in Chilean design codes were rarely enforced unless explicitly requested by owners, the 2010 Chile earthquake caused widespread damage to the suspended ceilings in all types of buildings [1, 2]; similarly, the 2011 Tohoku earthquake attacked the pacific coast of Japan with significant nonstructural damage. Post-earthquake reconnaissance and observations highlighted the damage to the suspended ceiling systems including the air conditioners and lighting fixtures, causing losses to structural functionality and economics [3].

Properly evaluating the seismic performance of suspended ceilings serves an essential role in estimating the building loss and the recoverability of building functions during an earthquake. To clarify the collapse mechanism and mitigate the drop-off damage of suspended ceiling systems, a series of full-scale shake table experiments of wide-area ceilings (defined in Japan as those with 200 m^2 or larger) were conducted in the E-defense laboratory [4]. The ceiling specimens were installed in a full-scale steel gymnasium with a mountain-shaped roof. According to the test results, collapse initiated by the up-lifting moment around the side wall in the case of conventional ceilings. For seismically designed ceilings, the failure mechanism depended on the balance of the strength of braces and metal connections between braces and the grid. Experimental observations revealed that metal clips connecting the steel runners were severely damaged by the horizontal and vertical excitations [5, 6].

However, those mentioned above and the other relevant researches [7-9] mainly examined the individual performance of suspended ceilings. Due to the difference in the dynamic characteristics, ceiling panels and electric equipment interact under earthquake excitations. Fig. 1(a) shows the collision damage between the ceiling panels and equipment. Another issue not fully examined in the previous researches is the seismic demand to the multi-elevation ceiling, whose conventional construction method has been reported [10] and implemented in practice occasionally.

(a) Collision between equipment and panels (b) At the step part in multi-elevation ceilings

Fig. 1 Damage of suspended ceiling system [3]

To elucidate the above issues, a series of vibration tests and shake table tests were conducted on the Japanese two-elevation integrated ceiling system, considering the interactions of ceiling panels with adjacent equipment. From the tests and corresponding numerical analyses, the general vibration characteristics of the equipment and integrated suspended ceiling system were obtained, and their seismic responses under earthquake excitations were analyzed in details.

2. Suspended Ceiling System

Suspended ceiling system is a widely-used nonstructural system in building structures, providing aesthetic appearance to conceal the overhead piping and mechanical systems. Typically, the electric equipment is installed and embedded into the ceiling panel blocks to meet the functional requirements.

The various construction configurations for ceilings exist between different countries. Fig. 2(a) presents the typical sketch of suspended ceiling components in the U.S., consisting of compression post, hanger wire, splay wire, and tee runner. In general, the lay-in panels are only placed on the flange of tee runners without any interactive fixed fastening; it is frequent to detect the isolated drop of ceiling panels due to the loose connection in the grid when subjected to earthquakes [11-13]. For the perimeter elements, pop rivets or screws often attach the grid members to the wall angles to ensure a reliable connection.

Ceiling system differs by countries and regions in several ways [14, 15]. In Japan, one of the most earthquake-prone countries, the ceiling system is characterized with: (1) threaded rods rather than wires for suspension of the constitutive grid; (2) diagonal metal braces as lateral restraints in two ways instead of splay wires in the seismic ceiling system; (3) a small gap of less than 5 mm between partitions and ceiling panels, filled by flexible sealing materials, to avoid any direct contact with the walls; (4) ceiling panels fixed with the runners by screws instead of merely placing on the flange of runners. The typical Japanese ceiling system is shown in Fig. 2b.

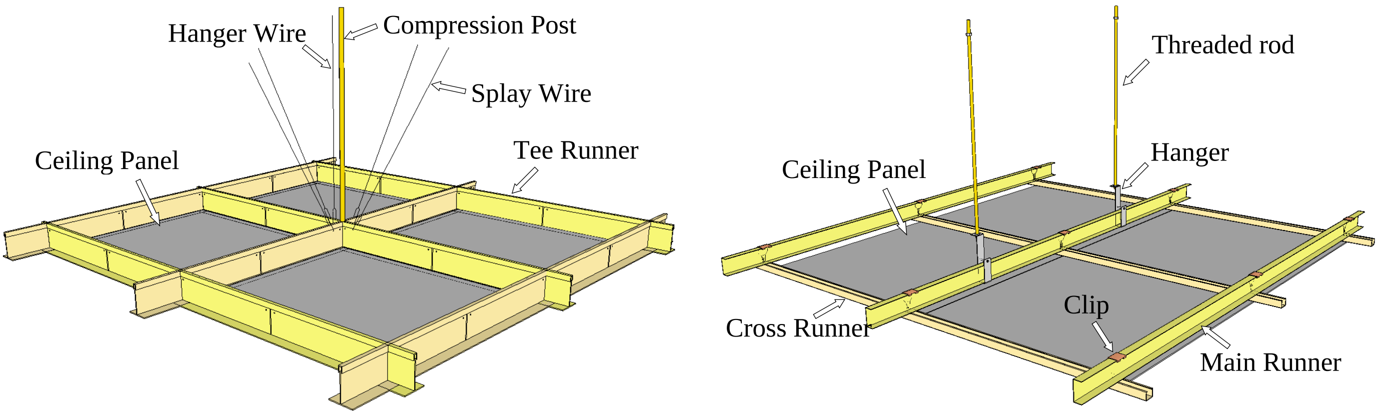

(a) U.S. ceiling system (b) Japanese ceiling system

Fig. 2 Typical ceiling system

3. Experimental Program

3.1 Test specimen

A steel frame with plan dimensions of 3.0 m×4.0 m and a height of 3.0 m was constructed and used to suspend the nonstructural components. The frame was firmly connected to the ground beam by M24 bolts, and the ground beam was fixed to the laboratory floor. The frame accommodated the lateral peripheral constraints representing walls at two different elevations. Diagonal braces were added to the frame to increase the stiffness of the entire steel frame. The cross-sectional dimensions of the frame members are listed in Table 1.

Experienced constructors installed the nonstructural components following field practices. Fig. 3(a) and Fig. 3(b) illustrate the specimen overview. Four units of electric equipment, namely, two air conditioners (ACs) and two lighting fixtures, were installed using suspension bars with two suspension lengths. Adjuster angles were used to adjust the distance between the suspension bars and the inserted hole in the floor slab. A clearance spacing existed between the equipment and the surrounding ceiling panels, similar to practice. The cross runners were connected with the main runners by clips, and the ceiling panels were fixed to the bottoms of the cross runners with self-drilling screws. Closely spaced supporting angles represented the slab of the top floor. Table 2 lists the critical properties of the entire ceiling system.

Table 1 Steel frame members

Structural component	Cross section (mm)
Column	□100×100×6
Beam (Top)	H-200×100×5.5×8
Peripheral boundary beam	C-150×75×20×4.5
Top supporting angle	∟-100×100×7
Brace	φ16

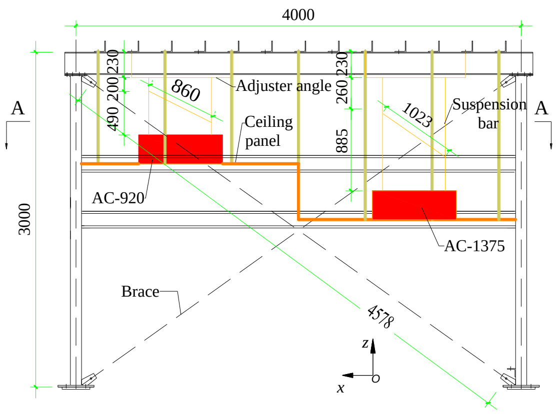

(a) Elevation view

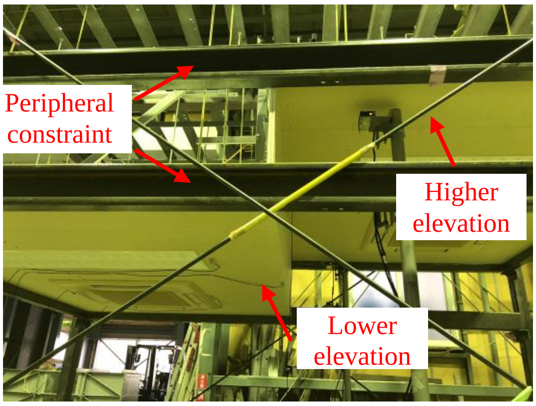

(b) Zoom-in on two elevations

Fig. 3 Test setup and specimen

Table 2 Ceiling components

Member	Size or thickness (mm)		Mass
Main runner	C-38×12×1.6		0.55 kg/m
Cross runner	C-19×25×0.5		0.28 kg/m
Suspension bar	φ9		0.50 kg/m
Clip	1.2		15.10 kg/m^2
Gypsum panel	22		0.04 kg/unit
AC	Body	840×840×258	22 kg/unit
	Cover	950×950×30	5 kg/unit
Lighting fixture	1279×332×121		7.7 kg/unit

3.2 Shaker loading test [16]

The test frame was excited by a shaker (APS-113, APS Dynamics) [17], which was firmly clamped to the center beam of the top floor. The maximum displacement stroke of the shaker was ±158 mm; hence, the shaker was able to provide enough dynamic excitation to vibrate the frame and the specimen. The ceiling panels and runners were installed and identified after the first measurements of the independent electric equipment.

The force with random white noise characteristics in the frequency range of 0.5-50 Hz was input in the x-direction to measure the natural frequencies and damping ratios of the entire system and its components. The peak acceleration of the input excitation was 0.01g. Each test case lasted 6 minutes, and the sampling rate of each measurement was 200 Hz. The test objectives are listed in Table 3.

Table 3 Test protocol for vibration test

Case	Components	Direction	Comments
1	Two ACs and two lighting fixtures	x	-
2	Integrated ceiling system (including the ceiling system, ACs, lighting fixtures)	x	With peripheral constraints
3	Integrated ceiling system (including the ceiling system, ACs, lighting fixtures)	x	Without peripheral constraints

Sixteen accelerometers were deployed to identify the dynamic properties of the ceiling panels, electric equipment, and steel frame.

3.3 Identification results

The modal characteristics of the integrated ceiling system, including its natural frequencies and corresponding damping ratios, were evaluated by the single-input-multi-output (SIMO) auto-regressive exogenous (ARX) model.

The identified vibration characteristics of each unit of electric equipment not surrounded by ceiling panels from Case 1 are shown in Table 4. The natural frequencies of AC-1375 and AC-920 decreased by 60% and 43%, respectively, after the diagonal braces were removed, showing a more pronounced reinforcing effect on the stiffness for equipment with a longer suspension length. The equipment with the shorter suspension bars had higher stiffness and frequency, and the 455 mm reduction in the suspension length for the lighting fixtures resulted in a 140% increase in the first frequency. No significant change in damping ratios was observed for different equipment. The damping ratio of each unit of electric equipment not surrounded by ceiling panels was only approximately 0.5%.

Table 4 Modal characteristics of the electric equipment (Case 1)

Component	AC-1375	AC-1375 w/o brace	AC-920	AC-920 w/o brace	Lighting-1375	Lighting-920
First frequency (Hz)	2.30	0.94	3.12	1.78	1.16	2.78
First modal damping ratio (%)	0.5	0.4	0.5	1.2	0.8	0.2

Table 5 lists the identification results of the integrated ceiling system. The diagonal braces of the ACs were installed throughout Cases 2 and 3. The natural frequencies of all components were almost the same, representing the coupled motion of adjacent components under small-amplitude shaking. The frequencies were almost six times larger with the peripheral boundary constraints than those without, indicating that the influences of the boundary conditions of nonstructural systems should be considered carefully during the design and assessment of integrated ceiling systems.

The ceiling panels had a relatively small damping ratio both with and without the peripheral constraints, i.e., 0.8% and 0.9%, respectively. In short, the damping ratio of the integrated ceiling system evaluated in this study can be set at 1.0%.

Table 5 Identification results of dynamic properties

Measurement location	With peripheral constraints		Without peripheral constraints	
	Frequency (Hz)	Damping ratio (%)	Frequency (Hz)	Damping ratio (%)
AC-1375	19.91	0.6	3.62	1.6
AC-920	19.23	1.6	3.55	1.0
Lighting-1375	19.38	2.6	3.53	1.0
Lighting-920	19.34	0.3	3.49	1.7
Ceiling-1375	19.45	0.4	3.47	1.2
Ceiling-920	19.02	1.5	3.51	0.9

Note: the value after the unit of electric equipment (AC or lighting fixture) is the corresponding suspension length.

3.4 Shake table test

A series of shake table tests were conducted to evaluate the seismic performance of the Japanese two-elevation integrated ceiling system. JMA Kobe ground motion was scaled into three levels, i.e., PGV 25 cm/s (Level 1), PGV 50 cm/s (Level 2), PGV 80 cm/s (Level 3), and then inputting the above motions into the overall structure. Fig. 4 shows the typical spectral characteristics of the JMA Kobe earthquake.

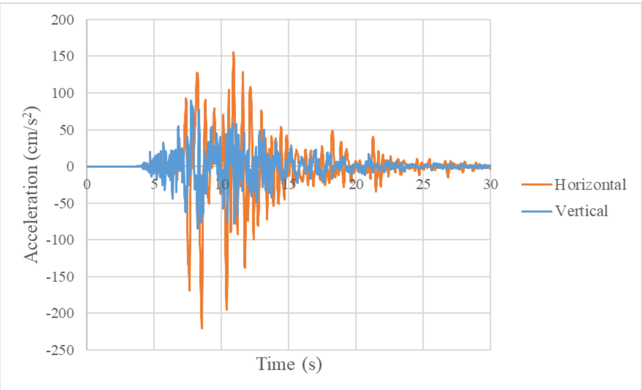

Fig. 4 Spectral characteristics of the input (PGV=25 cm/s)

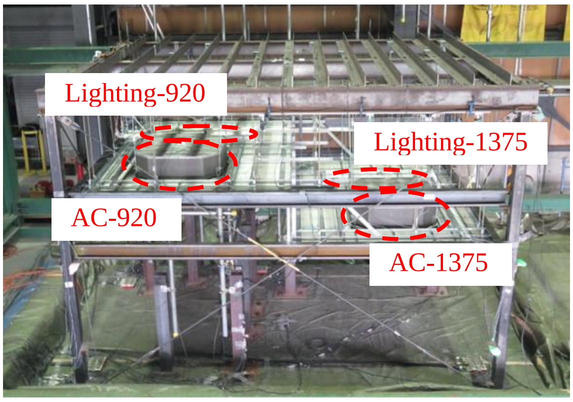

Fig. 5 Test overview

In total, 14 laser displacement transducers and 37 accelerometers were attached to different locations of the integrated system, including ceiling panels, ACs, Lightings, and piping. The on-site test configuration is shown in Fig. 5.

Under Level 1 and Level 2 excitations, sliding of both Lightings and ACs occurred, lightings moved more pronounced than ACs. Collision only took place between the two lightings and panels, while not around ACs. When subjected to JMA Kobe Level 3 earthquake, AC exhibited torsional deformation and the AC cover was stuck into the original clearance. Fig. 6 illustrates the typical damage in the ceiling system.

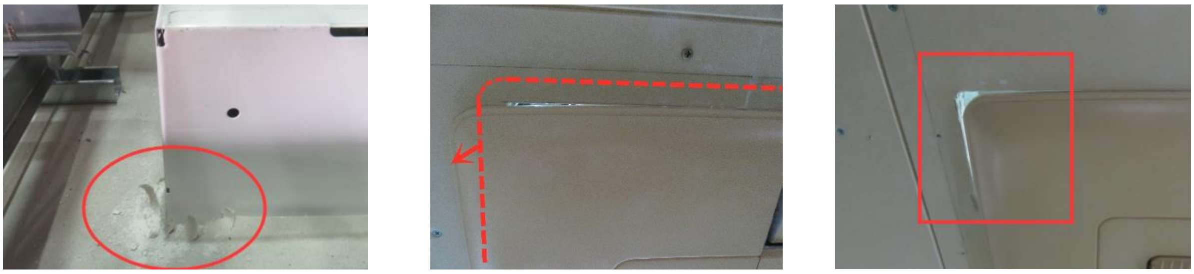

(a) Collision around lightings (b) Torsional deformation (AC) (c) AC cover stuck in the gap

Fig. 6 Damage observations

Furthermore, removing reinforcing bars decreases the overall stiffness of the integrated ceiling system. Almost the same response was shown on the two ceiling layers when the reinforcing bars were installed, while the relatively independent movement occurred for the two ceiling layers to some extent, as shown in Fig. 7.

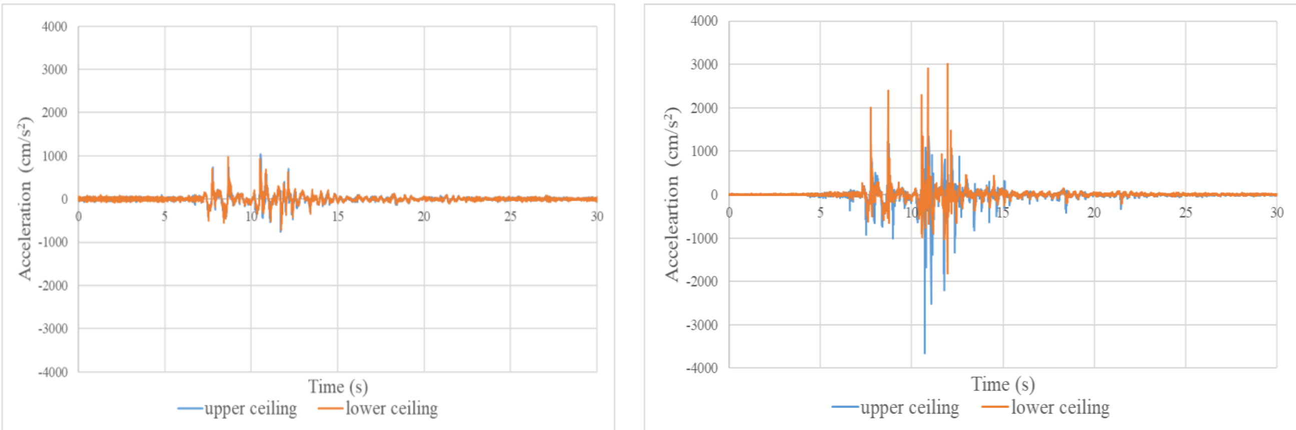

(a) With reinforcing bars (b) Without reinforcing bars

Fig. 7 Acceleration response of two ceiling layers

4. Numerical Investigation

To better understand the dynamic responses of the suspended integrated ceiling system, especially the coupled behavior of ceiling panels surrounded by equipment, further numerical studies were performed on the same integrated ceiling system.

4.1 Model establishment [16]

The steel frame was simplified as the supporting steel profiles and steel angles to represent the top floor; the four corners of the supporting frames were restrained at all degrees of freedom. The other components were constructed with the same properties as the experimental specimen, and the tops of the suspension bars were fixed to the steel frame. The steel grid was modeled using a series of beam elements with two different cross-sections for the main runners and cross runners. The connections between the main runners and cross runners were assumed to be rigid except for a relative horizontal stiffness of 349 N/mm considering the hangers. The overall model is shown in Fig. 8.

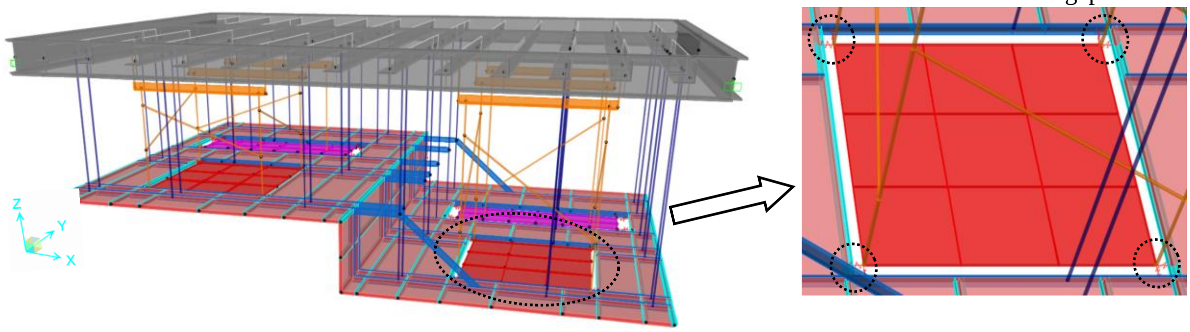

(a) Overview (b) Close-up view

Fig. 8 Integrated ceiling system model [16]

Rigid plate elements were used for the electric equipment, and the four corners of each equipment were connected with the suspension bar by pins. The diagonal braces and the vertical suspension bars on ACs were pin-connected as well, and the diagonal brace resisted only axial forces. Each unit of equipment was connected to adjacent panels by eight multilinear link elements, labeled henceforth as friction-gap elements, four of which were placed in the *x*-direction and the other four were in the *y*-direction.

Fig. 9 exemplifies a typical friction-gap element connecting an AC to the ceiling panel. The clearance between the AC and ceiling panel was 25 mm, and the clearance around the light was 5 mm, which is consistent with the installment practice. More specifically, friction was initially exhibited between the cover panel of the AC and the ceiling panel. After overcoming this frictional force, the relative displacement between the AC and the ceiling panel started to change. A collision occurred when the displacement reached the clearance between the AC and the ceiling panel, and then the stiffness increased to a huge number. The static frictional force was measured as 30N, which was determined by a tension test, and it was simplified and assumed to be the same as the sliding frictional force.

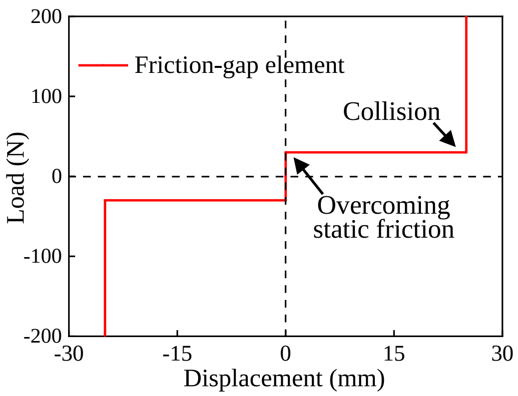

Fig. 9 Properties of typical friction-gap element [16]

4.2 FE verification

Modal analyses were performed both with and without peripheral boundary constraints, and the obtained numerical frequency results are listed in Table 6. The proposed model traced the shaker loading test results well, and the peripheral boundary constraints had a notable influence on the entire ceiling system, as witnessed in the tests.

Fig. 10 shows the first modal shape of the integrated ceiling system. It demonstrated that the existence of peripheral constraints serves a vital role in the vibration mode. Also, the friction-gap element makes a significant effect on the structural vibration of the integrated ceiling system. After removing the peripheral constraints, the first modal shape changes from the local vibration to the analogous floating system.

Table 6 Comparison between the numerical and shaker loading test results

	With peripheral constraints		No peripheral constraints	
	x-axis (Hz)	y-axis (Hz)	x-axis (Hz)	y-axis (Hz)
Test	19.38	16.62	3.53	2.68
FEM	19.63	15.94	3.15	2.68
Error (%)	1.3	4.1	10.8	0.1

Note: the experimental results are the mean values of the ARX identifications.

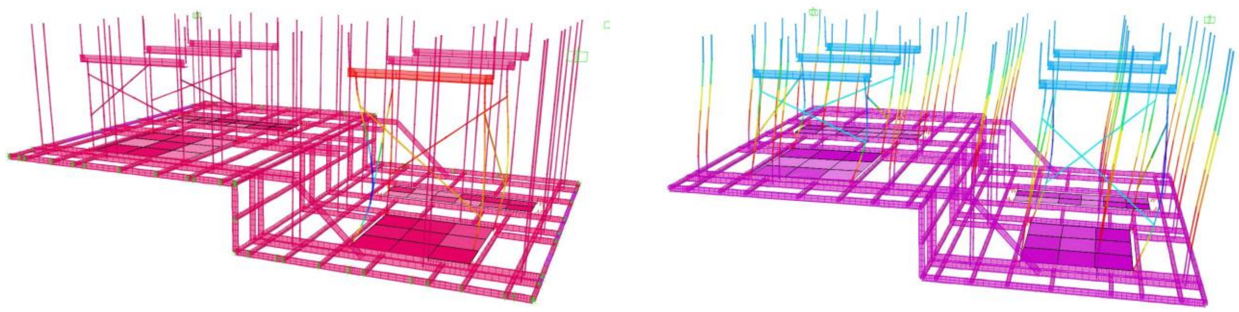

(a) With peripheral constraints (b) Without peripheral constraints

Fig. 10 First modal shape

Thus, to accurately estimate the seismic damage, it is imperative to model the interaction properties as realistic as possible.

4.3 Effect of reinforcing bars on dynamic properties

Typically, strengthening approaches are used between the two elevations. The main runners are extended over a certain distance, and inclined members are employed to connect the extended runners of the upper layer with the main runners at the lower elevation.

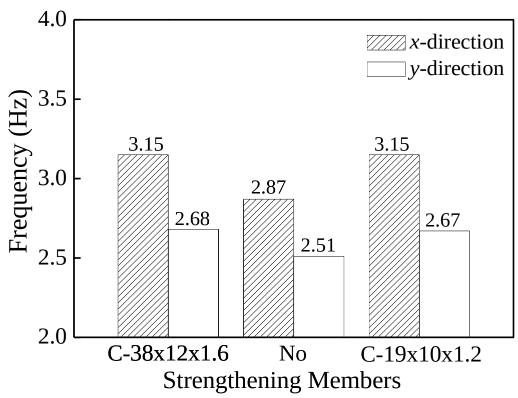

Fig. 11 First frequencies with different reinforcing members

Fig. 11 shows a comparison of the frequencies with different reinforcing members without boundary constraints. A smaller angle, C-19×10×1.2, was used to study the influence of reinforcing bars on the vibration properties of the integrated ceiling system. If peripheral constraints existed, the reinforcing bars at the rise-up location did not provide any contribution to either the horizontal or the vertical vibration characteristics. For the suspended ceiling system configuration without peripheral constraints, after eliminating the reinforcing members, the first horizontal vibration frequency decreased from 3.15 Hz to 2.87 Hz in the *x*-direction and from 2.68 Hz to 2.51 Hz in the *y*-direction. This result demonstrates that nearly 15% of the initial stiffness was reduced if no reinforcing bars existed at the rise-up location.

It can be concluded that reinforcing members at the rise-up location do not contribute to the vibration characteristics when peripheral constraints are present, while such members should be installed in integrated ceiling systems regardless of the member sections when these constraints do not exist.

4.4 Effect of peripheral constraints on equipment behavior

The seismic behavior of the two-elevation ceiling system with different peripheral constraints, labeled henceforth as Spec.wall (with peripheral constraints) and Spec.free (without peripheral constraints), were studied. The direct integration method was deployed to conduct time history analysis. The JMA Kobe ground motion, one set of the strongest records obtained from the 1995 Kobe earthquake with PGV scaled at 50 cm/s (NS-direction) and the corresponding UD-direction excitation, were inputted to investigate the specific nonlinear behavior of the integrated ceiling system. It corresponds to the extremely rare earthquake (approximately 500-year return period) in the Japanese seismic design code.

When the peripheral constraints are not present, the relative displacement between the two elevations is only 0.024 mm, indicating good integrity and no apparent damage to the overall system. However, unrecoverable deformation (16 mm) is shown on AC-920 (AC on the higher elevation), it proved that the components in the higher elevation should be more reinforced than those in the lower elevation. The displacement response of each equipment without peripheral constraints is shown in Fig. 12.

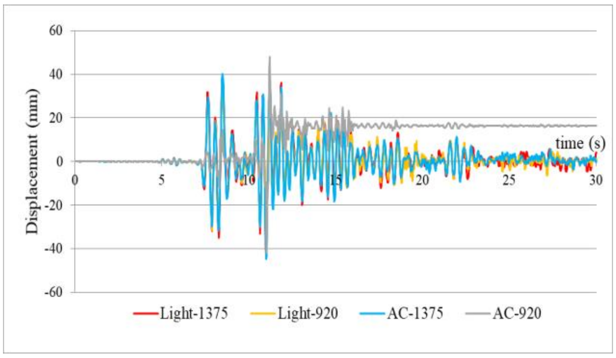

Fig. 12 Displacement of equipment (Spec.free)

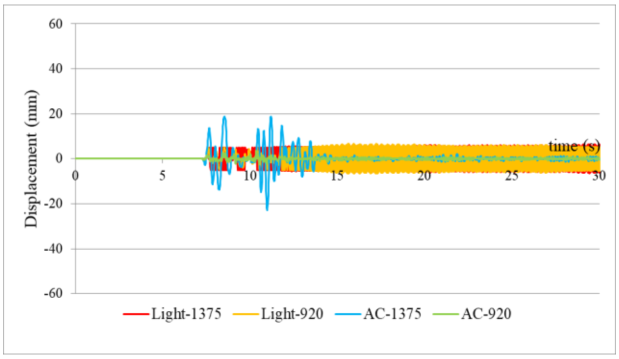

Fig. 13 Displacement of equipment (Spec.wall)

When the peripheral constraints existed, the movements of lighting fixtures reached the original clearance between the equipment and adjacent panels, showing the more flexible properties of lighting fixtures than ACs, shown in Fig. 13. Movement of AC-920 is the smallest because of its high lateral resistance, only less than 5mm.

5. Conclusions and Suggestions

The Japanese suspended ceiling system is somewhat different compared with the typical US ceiling. A series of vibration tests and shake table tests were conducted to understand the dynamic performance of the two-elevation integrated ceiling systems. The findings are summarized as follows:

1. In the vibration test, the damping ratio of the independent electric equipment not surrounded by ceiling panels was 0.5%, while the damping ratio of the integrated ceiling system considering such interactions increased to 1.0%.
2. For the integrated ceiling system, the peripheral constraints increased the first horizontal vibration frequency of the integrated ceiling system by a factor of six. Every unit of electric equipment moved together with the ceiling system due to the friction between the equipment and ceiling panels.
3. Friction-gap elements were proposed to model the connections between ceiling panels and equipment

considering the effects of friction and collision. The relative displacement between the AC and adjacent ceiling panels started to change after overcoming the frictional force. Then, the collision occurred, and the stiffness of the friction-gap element increased to infinity when the displacement reached the clearance between the AC and adjacent panel.

4. The reinforcing bar connecting two ceiling layers is beneficial to reduce the relative displacement and ensure the integrity of the integrated ceiling system.

Acknowledgments

The authors would like to thank the support provided by the Tokyo Metropolitan Resilience Project of the National Research Institute for Earth Science and Disaster Resilience (NIED) (Subject C, led by Masahiro Kurata). The financial support from Japan Society for the Promotion of Science (Grant No.19356) awarded the first author is highly appreciated as well.

References

[1] Miranda E, Mosqueda G, Retamales R, Pekcan G (2012): Performance of nonstructural components during the 27 February 2010 Chile earthquake. *Earthquake Spectra*, **28**(S1), S453-S471.

[2] Kato H, Tajiri S, Mukai T (2010): Preliminary reconnaissance report of the Chile Earthquake 2010. Tokyo, Japan: Building Research Institute.

[3] Architectural Institute of Japan (AIJ) (2012): Preliminary reconnaissance report of the 2011 Tohoku-Chiho Taiheiyo-Oki Earthquake. Tokyo: Maruzen Publishing.

[4] Sasaki T, Aoi A, Tagawa H, Kajiwara K, Araki T, Kanai T (2015): Collapse mechanism of wide-area suspended ceiling system based on e-defense full-scale shake table experiments. Tsukuba, Japan: National Research Institute for Earth Science and Disaster Prevention.

[5] Sasaki T, Aoi A, Kajiwara K, Tagawa H, Sato D (2017): Collapse mechanism of wide-area suspended ceiling based on full-scale shake table experiment of school gymnasium. *16th World Conference on Earthquake Engineering*, Santiago, Chile.

[6] Sasaki T, Aoi A, Kajiwara K, Tagawa H, Sato D (2016): Collapse mechanism of wide-area suspended ceiling in school gymnasium. *Proceedings of IASS Annual Symposia*, Tokyo, Japan.

[7] Yao Z, Liu Z (1996): Building structure test. Shanghai: Tongji University Press.

[8] Soroushian S, Rahmanishamsi E, Jenkins C, Maragakis EM (2019): Fragility analysis of suspended ceiling systems in a full-scale experiment. *Journal of Structural Engineering*, **145**(4), 04019005.

[9] Lu Y, Mosqueda G, Han Q, Zhao Y (2018): Shaking table tests examining seismic response of suspended ceilings attached to large-span spatial structures. *Journal of Structural Engineering*, **144**(9).

[10] Ministry of Land, Infrastructure, Transport and Tourism (MLIT) (2016): Construction guidelines for buildings. Tokyo: Public Buildings Association.

[11] Gilani AS, Reinhorn AM, Glasgow B, Lavan O, Miyamoto HK (2010): Earthquake simulator testing and seismic evaluation of suspended ceilings. *Journal of architectural engineering*, **16**(2), 63-73.

[12] Echevarria A, Zaghi A, Soroushian S, Maragakis M (2012): Seismic fragility of suspended ceiling systems. *15th World Conference on Earthquake Engineering (15WCEE)*, Lisbon, Portugal.

[13] Badillo-Almaraz H, Whittaker AS, Reinhorn AM (2007): Seismic fragility of suspended ceiling systems. *Earthquake Spectra*, **23**(1), 21-40.

[14] Sato Y, Motoyui S, Macrae G, Dhakal R (2011): Ceiling fragility of Japanese ceiling systems. *Proceedings of the Ninth Pacific Conference on Earthquake Engineering* Auckland, New Zealand.

[15] Qi L, Kunitomo K, Kurata M, Ikeda Y (2019): Proposal of vibration model considering interaction between ceiling system and equipment -part I: Experimental and numerical evaluation. *Summaries of Technical Papers of Annual Meeting Kinkin Brach*, Osaka, Japan.

[16] Qi L, Kunitomo k, Kurata M, Ikeda Y (2020): Investigating the vibration properties of integrated ceiling systems considering interactions with surrounding equipment. *Earthquake engineering & structural dynamics*, Accepted.

[17] Li X, Kurata M, Nakashima M (2015): Evaluating damage extent of fractured beams in steel moment-resisting frames using dynamic strain responses. *Earthquake engineering & structural dynamics*, **44**(4), 563-581.

